40.8% efficient inverted triple-junction solar cell with two independently metamorphic junctions

J. F. Geisz,[a] D. J. Friedman, J. S. Ward, A. Duda, W. J. Olavarria, T. E. Moriarty, J. T. Kiehl, M. J. Romero, A. G. Norman, and K. M. Jones
National Renewable Energy Laboratory, Golden, Colorado 80401, USA

(Received 12 August 2008; accepted 3 September 2008; published online 23 September 2008)

A photovoltaic conversion efficiency of 40.8% at 326 suns concentration is demonstrated in a monolithically grown, triple-junction III–V solar cell structure in which each active junction is composed of an alloy with a different lattice constant chosen to maximize the theoretical efficiency. The semiconductor structure was grown by organometallic vapor phase epitaxy in an inverted configuration with a 1.83 eV $Ga_{.51}In_{.49}P$ top junction lattice-matched to the GaAs substrate, a metamorphic 1.34 eV $In_{.04}Ga_{.96}As$ middle junction, and a metamorphic 0.89 eV $In_{.37}Ga_{.63}As$ bottom junction. The two metamorphic junctions contained approximately 1×10^5 cm^{-2} and $2-3\times10^6$ cm^{-2} threading dislocations, respectively. © *2008 American Institute of Physics*.
[DOI: 10.1063/1.2988497]

Currently available high-efficiency triple-junction solar cells consist of two III–V semiconductor junctions epitaxially grown lattice-matched on a single-crystal Ge substrate, which forms the bottom junction. This highly mature lattice-matched design has achieved 40.1% efficiency at 135 suns concentration[1] using $Ga_{.5}In_{.5}P$, $Ga_{.98}In_{.02}As$, and Ge junctions with the band gap combination of 1.86, 1.39, and 0.67 eV. By growing alloy layers with the same crystal lattice constant as the substrate, most dislocations, which form recombination sites (a loss mechanism), can be avoided. However, the constrained band gap combinations of the lattice-matched alloys are not optimal for maximum photovoltaic conversion efficiency of the solar spectrum. Using a semi-empirical model,[2] we have calculated the maximum theoretical efficiency of a series-connected triple-junction solar cell for a range of band gap combinations assuming GaAs-like material parameters. While it is unlikely that these actual theoretical efficiencies can be achieved, the relative values are instructive for optimizing a solar cell design. Figure 1 shows two calculated isoefficiency surfaces as a function of the three band gaps for the direct terrestrial spectrum under 500 suns concentration assuming a perfect antireflective coating (ARC).[3] The two-lobed shape is the result of the optical absorption of atmospheric water between 1300 and 1500 nm. These calculations show a global maximum efficiency for the band gap combination of 1.86, 1.34, and 0.93 eV, and a local maximum at 1.75, 1.18, and 0.70 eV that could be 5.2% and 4.9% (absolute) more efficient than the lattice-matched GaInP/GaInAs/Ge structure. The band gap combination (1.86, 1.39, and 0.67 eV) of the lattice-matched design is illustrated as a yellow cylinder in Fig. 1 for reference.

In order to grow a more efficient monolithic solar cell structure with an improved band gap combination, lattice-mismatched alloys with low defect densities are required. Compositionally graded buffer layers can be used to accommodate the lattice-mismatch by the formation of misfit dislocations within the buffer while inhibiting the propagation of these dislocations into the active junction. The resulting structure, incorporating active layers of different lattice constants separated by the graded layer, is commonly referred to as a metamorphic structure.[4]

Metamorphic triple-junction solar cells are beginning to realize their potential for higher efficiencies. An efficiency of 40.7% at 240 suns has been achieved[1] in a metamorphic triple-junction device using a Ge bottom junction and two coupled metamorphic junctions that are both 0.5% misfit from the substrate with the band gaps (1.80, 1.29, and 0.67 eV). This design (green cone in Fig. 1) approaches the lower maximum increasing the theoretical efficiency by 1.3% absolute, but its band gap combination is still far from optimized and some threading dislocations are introduced into the highest power producing top junction. Further decreasing the top two junction band gaps with this approach is very

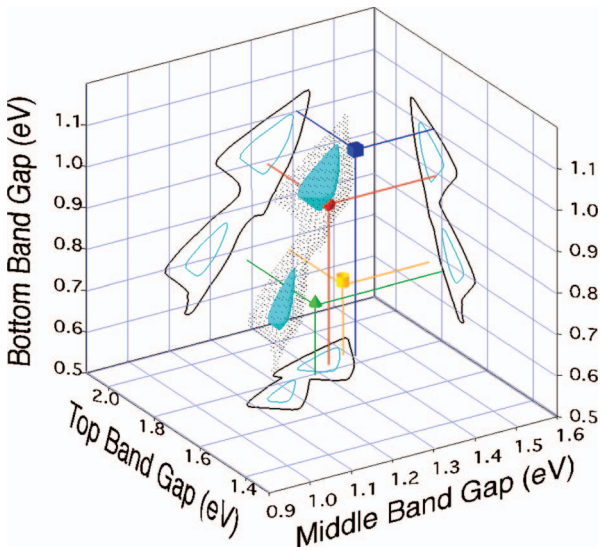

FIG. 1. (Color) Theoretical isoefficiency surfaces and their projected contours for series-connected triple-junction solar cells under the direct terrestrial solar spectrum at 500 suns concentration: 51% (black) and 52% (light blue). Band gap combinations of actual champion devices are also shown: (1.86, 1.39, and 0.67 eV), yellow cylinder; (1.80, 1.29, and 0.67 eV), green cone; (1.84, 1.41, and 1.00 eV), dark blue cube; and (1.83, 1.34, and 0.89 eV), red sphere.

[a]Electronic mail: john_geisz@nrel.gov.

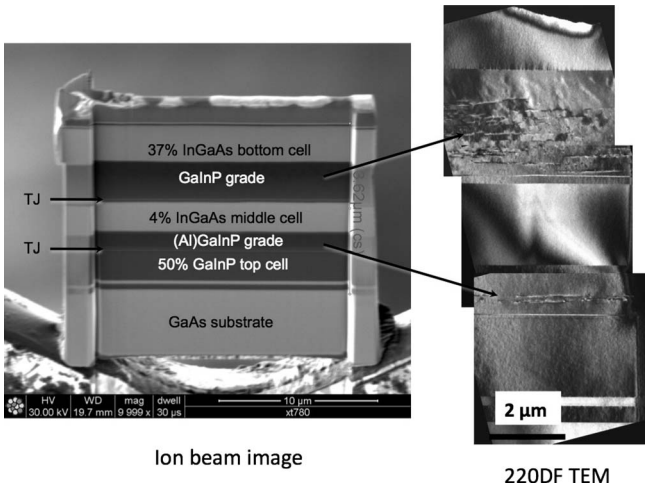

FIG. 2. Ion beam image and composite 220 dark-field TEM of a FIB cross-section of an unprocessed inverted triple-junction solar cell structure.

difficult because the performance is very sensitive to dislocations in the top GaInP junction. By inverting the direction of growth and removing the substrate, a device with two high-quality lattice-matched top junctions, $Ga_{.5}In_{.5}P$ and GaAs, and a highly lattice-mismatched (1.9% misfit) $In_{.27}Ga_{.73}As$ bottom junction with band gaps (1.84, 1.41, and 1.00 eV) can be grown on GaAs substrates that increases the theoretical efficiency by 3.1% relative to the lattice-matched design on Ge. This inverted design (dark blue cube in Fig. 1) has many other advantages over the more conventional triple-junction designs that utilize a Ge bottom junction.[5,6] We have previously demonstrated 39.2% efficiency at 131 suns concentration[7] and 33.8% efficiency under AM1.5 global conditions[6] with this inverted design containing a single metamorphic junction. In this letter, we demonstrate an improved inverted triple-junction solar cell with nearly optimized band gaps (1.83, 1.34, and 0.89 eV) utilizing two independently metamorphic junctions. The band gaps of this improved inverted design, shown as a red sphere in Fig. 1, closely approach the theoretical global maximum. We demonstrate here a performance of 40.8% efficiency at 326 suns for this design, but further development could potentially boost the efficiency by over 4% (absolute) beyond that of the lattice-matched design.

The structure of the inverted triple-junction device is pictured in Fig. 2. It was grown by atmospheric-pressure organometallic vapor phase epitaxy on a (001) GaAs substrate miscut 2° toward (111)B. The top 1.83 eV $Ga_{.51}In_{.49}P$ junction was grown first, lattice-matched to the GaAs substrate. The middle 1.34 eV $In_{.04}Ga_{.96}As$ junction was grown next after gradually increasing the lattice constant by 0.3% with an (Al)GaInP step-grade. Finally, the bottom 0.89 eV $In_{.37}Ga_{.63}As$ junction (2.6% misfit) was grown after further increasing the lattice constant with a GaInP step-grade. All junction thicknesses were about 2.5–2.9 μm. Because nearly optimal band gaps were used, current-matching was achieved without the need to thin any junctions. The grades were designed to be transparent to the light required in the junctions below them and to achieve near-zero strain within the active junctions.[8,9] Each *n*-on-*p* homojunction was clad with passivating window and back-surface-field layers of an (Al)GaInP composition with higher band gap than the junction but identical lattice constant. Tunnel junctions (TJs) were grown between each junction before the graded layers. The TJ between the top and middle junction was thus lattice-matched to the top junction and the substrate, but the TJ between the middle and bottom junction was grown on the metamorphic middle junction. This thin metamorphic TJ consisted partly of the $In_{.04}Ga_{.96}As$:Se that matched the metamorphic middle junction lattice constant that it was grown on, but also $Al_{.3}Ga_{.7}As$:C that was grown in tension on the metamorphic middle junction. Carbon doped $In_{.04}Ga_{.96}As$ was not used because In-containing alloys are difficult to dope with carbon. While this TJ design is less than ideal because of the strained AlGaAs layer, it provided low-resistance Ohmic-like conduction in the device up to 826 suns concentration. At higher concentrations, the photocurrent of the device exceeded the peak tunneling current of the TJ, as evidenced by the appearance of the characteristic tunneling signature in the current-voltage curves.

A semiconductor structure identical to the one processed for solar cell measurements was analyzed for structural properties. X-ray diffraction analysis showed the metamorphic junctions to be in only 0.029% and 0.014% compressive strain. Plan-view, spectrally resolved cathodoluminescence images indicated approximately 1×10^5 cm^{-2} and $2-3\times10^6$ cm^{-2} threading dislocations in the middle and bottom junctions, respectively. The threading dislocations in the top junction were below the detection limit (5×10^4 cm^{-2}). The focused ion beam (FIB) section shown in Fig. 2 was imaged by transmission electron microscopy (TEM). The (220) dark-field images, also in Fig. 2, clearly show many dislocations within the two graded buffer layers, but almost none in the three active junction regions. Only one dislocation was observed in the bottom junction in the entire 30 μm of the two sections viewed by TEM. The dislocation density in this 0.89 eV bottom junction was comparable to that in our 1.0 eV junctions[8] and the dislocation density in the 1.34 eV middle junction was low enough to have almost negligible impact on performance.[10]

The inverted device was processed as described previously.[6] The gold back contact was applied, the inverted structure bonded to a silicon handle with epoxy, the GaAs substrate removed, the front metal grids applied, the devices isolated, and an ARC deposited. Se-doped GaInNAs was used as a top contact layer in the inverted structure to reduce the contact resistance with the gold grids. The presence of the nitrogen appears to inhibit Se diffusion from the contact layer during the growth of the remainder of the structure,[11] as well as increase the maximum carrier concentration.[12] The external quantum efficiency (QE) of each junction was measured separately by light biasing the other two junctions.[13] Current-voltage (*IV*) measurements were taken under a continuous multisource solar simulator adjusted to the appropriate one-sun spectrum using three individual single-junction reference cells.[13] High irradiance *IV* measurements were taken under a flash simulator. The flash lamp voltage was adjusted to try to match the current ratio of the two most current limiting junctions to the AM1.5 direct spectrum (low aerosol optical depth[14]) spectrum, in this case the middle and bottom junctions.

The external QE and reflectance of the device are shown in Fig. 3. The currents of all three junctions, given by the integral of the QE times the spectrum, were the same within the uncertainty of the measurement. The *IV* measurements of

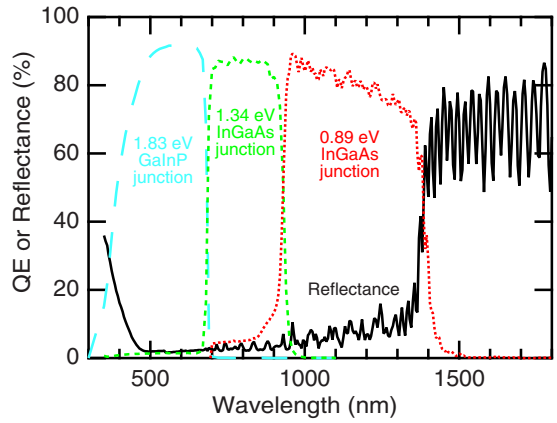

FIG. 3. (Color online) External QE and specular reflectance of inverted triple-junction solar cell.

a 0.25 cm^2 device measured under the AM1.5 global (IEC 60904) conditions resulted in an open circuit voltage (V_{oc}) of 2.79 V, short circuit current density (J_{sc}) of 13.9 mA/cm^2, fill factor of 85% and efficiency of 33.2%. Under concentration, the efficiency of a 0.1 cm^2 device reached 40.8% at an irradiance of 326 kW/m^2 (or 326 suns) as shown in Fig. 4. At this irradiance, the V_{oc} was 3.28 V and the fill factor was 88.4%. The efficiency was maintained to 39.2% out to 841 suns, but dropped dramatically thereafter because the current exceeded the peak tunneling current of one of the TJs.

The actual band gap of the bottom junction was chosen slightly lower than the theoretical optimum because of practical considerations. Current loss in the bottom junction relative to the top two junctions was caused by significant reflectance in the infrared. Lowering the bottom junction band gap resulted in sufficient current to match the series-connected currents of the other junctions, but resulted in slightly lower voltages than could be achieved with a perfect ARC. The development of an ultrabroadband ARC would improve this situation.

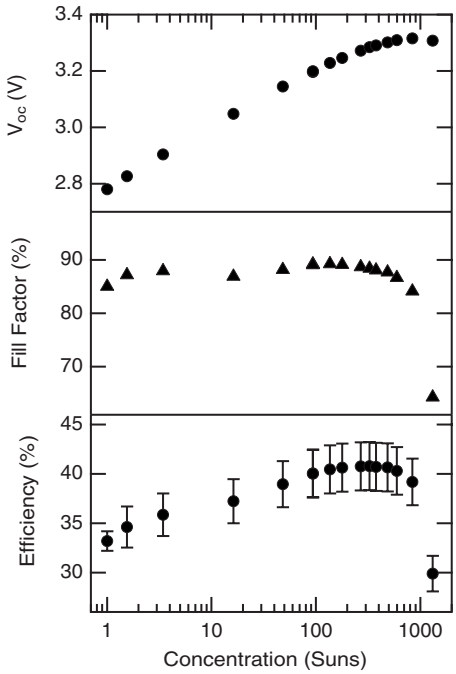

FIG. 4. V_{oc}, fill factor, and efficiency of the inverted triple-junction device under the direct terrestrial spectrum as a function of concentration.

In summary, a triple-junction solar cell utilizing alloy compositions with three different lattice constants within the active regions of a single monolithically grown III–V semiconductor structure has been demonstrated. This allowed for the complete optimization of the three junction band gaps for maximum efficiency. While III–V photovoltaic junctions are very sensitive to threading dislocations, the dislocation densities within the two metamorphic junctions were low enough to result in a net improvement in efficiency beyond any other solar cell reported.

The authors thank M. Young, C. Kramer, and K. Emery for their contributions. We also thank Sarah Kurtz, J.M. Olson, and M.W. Wanlass for useful discussions and their pioneering work that made this possible. This work was funded by the United States Department of Energy under Contract No. DE-AC36-99-GO10337.

[1]R. R. King, D. C. Law, K. M. Edmondson, C. M. Fetzer, G. S. Kinsey, H. Yoon, R. A. Sherif, and N. H. Karam, Appl. Phys. Lett. **90**, 183516 (2007).
[2]D. J. Friedman, J. F. Geisz, A. G. Norman, M. W. Wanlass, and S. R. Kurtz, *Proceedings of the Fourth World Conference on Photovoltaic Energy Conversion*, Hawaii (IEEE, New York, 2006), p. 598.
[3]Slightly higher absolute theoretical efficiencies were calculated here than in Ref. 2 because it assumed an empirical two-layer ARC, but the positions of the maxima remain essentially unchanged.
[4]D. E. Grider, S. E. Swirhun, D. H. Narum, A. I. Akinwande, T. E. Nohava, W. R. Stuart, and P. Joslyn, J. Vac. Sci. Technol. B **8**, 301 (1990).
[5]M. W. Wanlass, S. P. Ahrenkiel, R. K. Ahrenkiel, D. S. Albin, J. J. Carapella, A. Duda, J. F. Geisz, S. Kurtz, T. Moriarty, R. J. Wehrer, and B. Wernsman, *Proceedings of the 31st IEEE Photovoltaic Specialists Conference*, Orlando, Florida (IEEE, New York, 2005), p. 530.
[6]J. F. Geisz, S. Kurtz, M. W. Wanlass, J. S. Ward, A. Duda, D. J. Friedman, J. M. Olson, W. E. McMahon, T. E. Moriarty, and J. T. Kiehl, Appl. Phys. Lett. **91**, 023502 (2007).
[7]J. F. Geisz, S. Kurtz, M. W. Wanlass, J. S. Ward, A. Duda, D. J. Friedman, J. M. Olson, W. E. McMahon, T. E. Moriarty, J. T. Kiehl, M. J. Romero, A. G. Norman, and K. M. Jones, *Proceedings of the 33rd IEEE Photovoltaic Specialist Conference*, San Diego (IEEE, New York, 2008).
[8]J. F. Geisz, A. X. Levander, A. G. Norman, K. M. Jones, and M. J. Romero, J. Cryst. Growth **310**, 2339 (2008).
[9]S. P. Ahrenkiel, M. W. Wanlass, J. J. Carapella, L. M. Gedvilas, B. M. Keyes, R. K. Ahrenkiel, and H. R. Moutinho, J. Electron. Mater. **33**, 185 (2004).
[10]C. L. Andre, A. Khan, M. Gonzalez, M. K. Hudait, E. A. Fitzgerald, J. A. Carlin, M. T. Currie, C. W. Leitz, T. A. Langdo, E. B. Clark, D. M. Wilt, and S. A. Ringel, *Proceedings of the 29th IEEE Photovoltaic Specialists Conference*, New Orleans, Louisiana (IEEE, New York, 2002), p. 1043.
[11]M. A. Steiner, J. F. Geisz, R. C. Reedy, and S. Kurtz, *Proceedings of the 33rd IEEE Photovoltaic Specialist Conference*, San Diego (IEEE, New York, 2008).
[12]K. M. Yu, W. Walukiewicz, W. Shan, J. W. Ager, J. Wu, E. E. Haller, J. F. Geisz, D. J. Friedman, and J. M. Olson, Phys. Rev. B **61**, R13337 (2000).
[13]K. Emery, M. Meusel, R. Beckert, F. Dimroth, A. Bett, and W. Warta, *Proceedings of the 28th IEEE Photovoltaic Specialists Conference*, Anchorage, Alaska (IEEE, New York, 2000), p. 1126.
[14]K. A. Emery, D. Myers, and S. Kurtz, *Proceedings of the 29th Photovoltaics Specialists Conference*, New Orleans (IEEE, New York, 2002), p. 840.